Mach-Zehnder Interferometer and Essential Photonics Components Performance Investigation

Xia Fang

***Abstract*— This report describes the design of imbalanced Mach-Zehnder interferometer with different lengths. Also include a 1550nm grating to check the transmission and reflection spectrum with 2X2 couplers.**

***Index Terms*—Mach-Zehnder Interferometer (MZI), grating, coupler, Y-branch**

I. INTRODUCTION

SILICON photonics allows low-cost compact and energy efficient components for high-speed data and communication sensors. The Mach-Zehnder interferometer, gratings, coupler, ring resonators are essential blocks for modern optical networks. [1,2]

In this report, I provide some theoretical background for the essential photonics passive components, and the simulation results of imbalanced MZI with different arm lengths. We also compare the simulation results and measurement results and analysis of the differences, which can help us to better understand the performance of different photonics devices and the fabrication variation.

II. THEORY

A. Mach_Zehnder Interferometer

Mach-Zehnder interferometer is a device that consists of two couplers connected by two optical phases with different optical phases. When light recombines at the second coupler, constructive or destructive interference occurs depending on the phase difference between the two arms. There are several important parameters that are useful to elevate the MZI performance. The most important one is the free spectrum range (FSR), which is determined by the operation wavelength, length difference of two arms and group index

$$\mathrm{FSR} = \Delta\lambda = \frac{\lambda^2}{\Delta L\left(n - \lambda\frac{dn}{d\lambda}\right)} = \frac{\lambda^2}{\Delta L n_g} \qquad (1)$$

The FSR can be measured from the output interference spectrum from MZI, which is the distance between two adjacent peaks or dips. From the measurement result and the known length difference of two arms, we can get the group index which is defined as:

$$n_g = n - \lambda\frac{dn}{d\lambda}. \qquad (2)$$

It can be calculated if we know the wavelength dependence of refractive index, which is associated with dispersion. It can be obtained from commercial software, such as Ansys Lumerical.

The group index can also be defined as the ratio of the vacuum velocity of light to the group velocity in the medium. So, it is used to describe how fast an optical pulse can travel through the medium which is related to information transfer. However, the refractive index is defined as the ratio of the speed of light in a vacuum to the phase velocity, and it is a function of the material’s properties, including its permittivity and permeability. The phase velocity of a wave is the speed of any surface of constant phase (wavefront: set of points having the same phase). The Phase velocity is not a physically meaningful quantity and is not related to information transfer.

$$n = c / v_p = ck / \omega.$$

The output power of the interferometer is determined by this equation

• Imbalanced interferometer, with identical waveguides:

$$I_o = \frac{I_i}{2}\left[1 + \cos\left(\beta\Delta L\right)\right]$$

Where the beta is the propagation constant of light which is defined by:

The propagation constant of a sinusoidal electromagnetic wave is a measure of the change undergone by the amplitude and phase of the wave as it propagates in each direction.

$$\beta = \frac{2\pi n}{\lambda}$$

By measuring the output interference spectrum, we can get a lot of information. Such as FSR, extinguish ratio. The arm length difference of MZI should be carefully chosen to make sure the output spectrum covers enough fringes and at mean time the peaks are not too close to each other due to the resolution limitation of spectrum analyzer. The extinction ratio (ER), or essentially the visibility of interference fringe depends on the loss difference between the two arms. So, with known length difference, we can get the waveguide loss/length by measuring the ER through this equation:

$$\Rightarrow ER = 10\log_{10}\frac{T_{max}}{T_{min}} = 20\log_{10}\left(\frac{1+10^{-IL/20}}{1-10^{-IL/20}}\right)$$
$$\sim 20\log_{10}\left(\frac{40}{IL\cdot\ln 10}\right)$$

Compared to the cutback method, use MZI to measure the propagation loss of the tested device is inherently insensitive to any coupling coefficient variation in the measurement.

B. *Bragg Gratings:*

The silicon photonics Bragg grating has a periodic perturbation of the refractive index along the waveguide structure. By tuning the pitch, it can affect the effective refractive index and changes the resonant wavelength, which

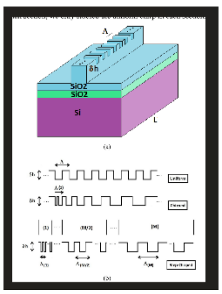

is defined as:

$$\lambda_B = 2\, n_{eff}\, \Lambda$$

Where the Λ is grating pitch. The resonant wavelength. In this design, a 1550nm Bragg grating (TE) is included to investigate both transmission and reflection performance. The input power will split 5:5, 50% power will go to the grating for transmission and reflection spectrum, other 50% power will be coupled back to detector as a reference background spectrum which will be used to substrate the grating's transmission/reflection spectrum to get the pure gratin's spectra.

C. *Waveguide coupler*

There are four commonly used coupler designs in silicon photonics: directional coupler, multimode interferometer (MMI), adiabatic coupler ,and Y-branch. Directional coupler is a passive device that has two waveguides

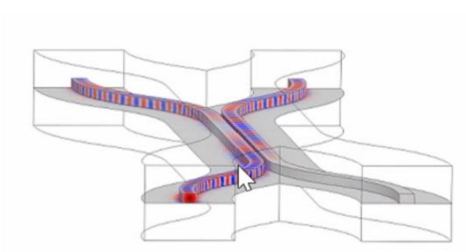

Directional coupler

brought close to each other. The power transfer between two waveguides through evanescent interactions. The power coupling ratio is determined by the gap between the two waveguide ,and coupling length. A directional coupler has a quite straightforward design; it is quite sensitive to operation wavelength as well as fabrication variations. The MMI is a device that light goes into a wide multimode section, and then through a beating between the multiple orders of transvers modes in this section, then redistribute the output into multiple waveguides. Mechanism. Adiabatic coupler is a device that has gradual (adiabatic) transformation of optical mode from one waveguide to another, typically through tapered geometry or supermodel evolution. It has very broadband range, as it dose need

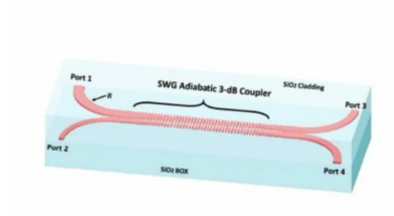

Adiabatic coupler

phase matching requirement (no interference), it is widely used as fiber-chip edge coupler and wavelength-insensitive splitters. Y-branch is a device that input waveguide splits gradually into two branches (like a Y), dividing political power geometrically. It is simple design and easy to fabricate but tends to suffer from reflection and loss at the junction if not tapered adiabatically (gradually). It is broadband but limited uniformity between outputs if asymmetrical.

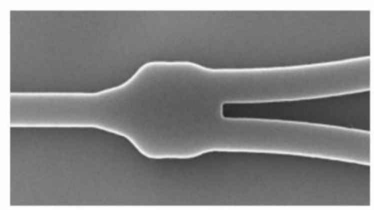

Y-junction

D. *Ring resonator*

An Optical ring resonator is a closed-loop waveguide (ring or racetrack shape) that traps light when the round-trip phase condition is satisfied:

$$m\lambda = n_{\text{eff}} L$$

Where L is the ring circumference and m is an integer. There are two main types of optical resonators: all pass resonator and add drop resonator. The resonator is used for filters, phase shifters, and optical delay lines.

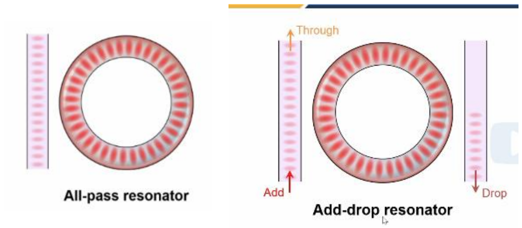

The qualify factor (Q factor) of a resonator describes how efficiently it stores energy, and how long light circulates before its energy decays.

$$Q = \omega_0 \frac{\text{Energy Stored}}{\text{Power Loss per Cycle}}$$

The Q factor is also defined equivalently by:

$$Q = \frac{\lambda_0}{\Delta\lambda}$$

Where:

- $\omega_0 = 2\pi c/\lambda_0$ = angular resonance frequency
- λ_0 = resonant wavelength
- $\Delta\lambda$ = full-width at half maximum (FWHM) of the resonance dip/peak

High Q means the light circulates many round trips before decaying, and the loss of resonators is very low. The resonator has narrow linewidths. The Q factor also corresponds to how long a photon stays in the cavity before it is absorbed or coupled out. High Q means long photon lifetime, and vice versa. Therefore, high Q resonator has very sharp resonance, and excellent wavelength filtering or sensing resolution.

The total Q is limited by intrinsic losses (material, scattering, absorption) and coupling losses.

$$\frac{1}{Q_{total}} = \frac{1}{Q_{int}} + \frac{1}{Q_{cpl}}$$

- Q_{int}: intrinsic Q, limited by propagation loss inside the ring
- Q_{cpl}: coupling Q, controlled by the gap between ring and bus

The high Q resonator is good for filtering and sensing ,while low Q resonator is for faster modulation because low Q means the shorter photo-lifetime, and the photons can leave cavity sooner.

The FSR (free spectrum range) is defined as the same as MZI.

$$FSR = \frac{\lambda_0^{\,2}}{n_g L}$$

III. Design and Simulation Results

There are four different devices in the designs, and all of them are in TE mode. The MZI1and MZI3 are simple Mach Zander interferometers with different length delta. Both MZI1 and MZI3 uses the broadband coupler. It is a specific type of tapered directional coupler. It is a hybrid engineered coupler designed to be wavelength-insensitive across a broad band. 2

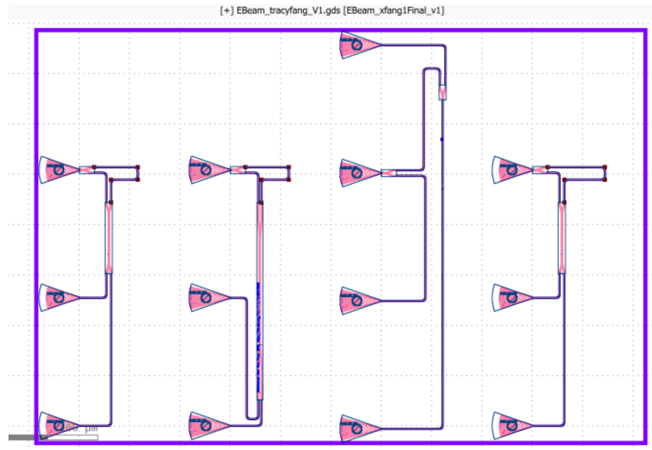

The MZI2 is the same as MZI1(length delta in two MZI differs slgihtly~0.1um), except the output coupler is adiabatic coupler which has very long taper length. The length delta in MZI1 and MZI2 are both 60um, while MZI3 has length difference of 88um.

By using the Lumerica and setting the simulation wavelength range from 1.5um to 1.6um. The output interference spectrum from MZ1 is shown as below.

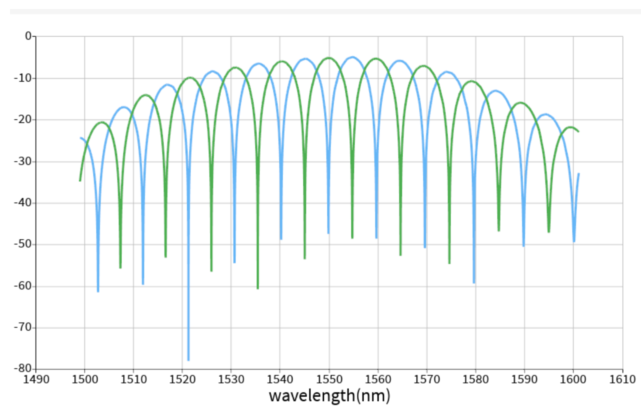

The simulated FSR is 9.6 nm. With the known value of length difference: 60um, we can calculate the group index Ng= (1.55) ^2/60/9.6*10^3=4.2 based on the equation (1). The calculated group index matches the simulation result from Lumerical MODE:

mode #	effective index	wavelength (µm)	loss (dB/cm)	group index	TE polarization fraction (Ex)	waveguide TE/TM fraction (%)	effective area (µm^2)
1	2.446821+1.249901e-09i	1.55	0.00044009	4.203676+2.666269e-09i	98	76.12 / 81.96	0.190575
2	1.768817+8.502991e-10i	1.55	0.00029939	3.720462+4.417991e-09i	4	68.93 / 88.89	0.368811
3	1.496336+5.049426e-10i	1.55	0.00017779	2.459976+3.434186e-09i	65	86.51 / 96	0.826491

Here is simulated beam profile from 500nm width, 220nm height silicon-based waveguide at 1550nm.

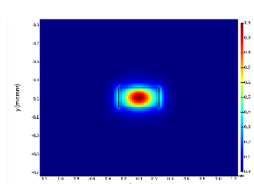

Here is the simulation result of MZI2 with an adiabatic output coupler. The output interference pattern is very similar to that of the MZI with a broadband coupler. The slightly fringe shift is due to path-length difference between the two arms differs slightly (~0.1um) ar

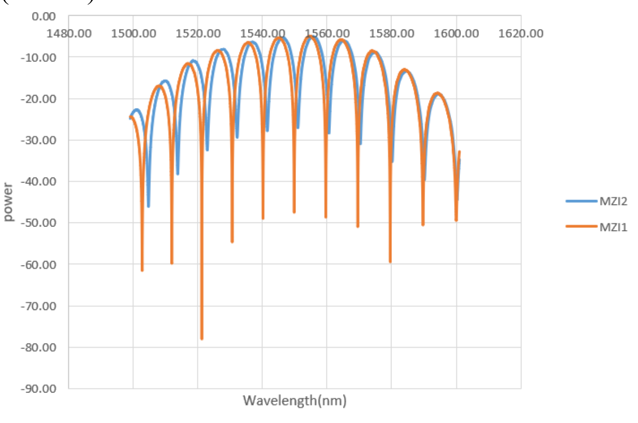

The table below compares the MZI1, MZI2,MZI3 with different delta of two arms. The FSR Is shorter when length difference is larger. The calculated group indexes of three MZI are close to the simulation result from MODE.

TE1550	Length delta(um	FSR (nm)	Ng
MZI1	60.02	9.6	4.169617072
MZI2	59.94	9.5	4.219131412
MZI3	87.89	6.5	4.205431615

VI. MEASUREMENT VS SIMULATION

The photonic devices were fabricated using the NanoSOI MPW fabrication process by Applied Nanotools Inc. (http://www.appliednt.com/nanosoi; Edmonton, Canada) which is based on direct-write 100 keV electron beam lithography technology. Silicon-on-insulator wafers of 200 mm diameter, 220 nm device thickness and 2 µm buffer oxide thickness are used as the base material for the fabrication. The wafer was pre-diced into square substrates with dimensions of 25x25 mm, and lines were scribed into the substrate backsides to facilitate easy separation into smaller chips once fabrication was complete. After an initial wafer clean using piranha solution (3:1 H_2SO_4:H_2O_2) for 15 minutes and water/IPA rinse, hydrogen silsesquioxane (HSQ) resist was spin-coated onto the substrate and heated to evaporate the solvent. The photonic devices were patterned using a JEOL JBX-8100FS electron beam instrument at The University of British Columbia. The exposure dosage of the design was corrected for proximity effects that result from the backscatter of electrons from exposure of nearby features. Shape writing order was optimized for efficient patterning and minimal beam drift. After the e-beam exposure and subsequent development with a tetramethylammonium sulfate (TMAH) solution, the devices were inspected optically for residues and/or defects. The chips were then mounted on a 4” handle wafer and underwent an anisotropic ICP-RIE etch process using chlorine after qualification of the etch rate. The resist was removed from the surface of the devices using a 10:1 buffer oxide wet etch, and the devices were inspected using a scanning electron microscope (SEM) to verify patterning and etch quality. A 2.2 µm oxide cladding was deposited using a plasma-enhanced chemical vapour deposition (PECVD) process based on tetraethyl orthosilicate (TEOS) at 300ºC. Reflectometry measurements were performed throughout the process to verify the device layer, buffer oxide and cladding thicknesses before delivery.

A. Measurement result of MZI1

The measured FSR from MZI1 at 1550nm is about 9.65 which is slightly larger than the simulation result, while the group

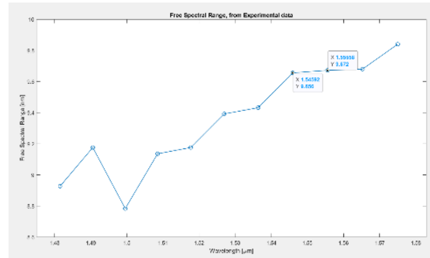

index is 4.16 which is very closer to the simulation result. It

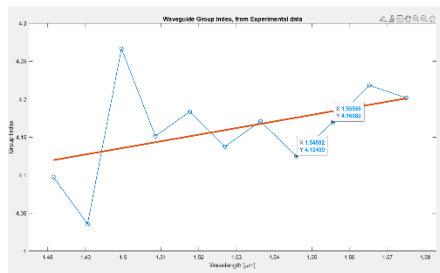

indicates that arms’ length difference deviates slightly from the design due to the fabrication variation. The manufacturing challenges in silicon photonics commonly arise from variations in silicon thickness, feature dimensions, and the smoothing of lithography and etching processes. There are a lot of factors that can cause fabrication variation, such as the resist degradation, exposure dose fluctuations, development time variations, and changes in chemical age or composition. All these can significantly impact device performance because they alter the physical geometries of photonics structures and change the optical propagation path.

IV. CONCLUSION

In this work, I investigated the performance of Mach-Zehnder interferometers (MZIs) and several essential photonic components through a combined analytical, numerical, and experimental study.

Comprehensive simulations were carried out using MODE and INTERCONNECT from Ansys Lumerical, which enable accurate predication of MZI spectrum response. Experiments performed on fabricated devices showed an FSR of ~9.5nm at 1550nm, which closely matches the simulation results. Minor deviations between measured and simulated spectra were primarily attributed to fabrication-induced variations such as waveguide width and thickness non-uniformity, etch process variation, lithography smoothing, and slight discrepancies in path length.

Overall ,the strong agreement between simulation and measurement validates both the theoretical derivations and the robustness of the design approach. The results demonstrate that well-designed silicon photonic MZIs can achieve predictable and stable spectral performance, even in the presence of typical fabrication tolerances.

Acknowledgment

I acknowledge the edX UBCx Phot1x Silicon Photonics Design, Fabrication and Data Analysis course, which is supported by the Natural Sciences and Engineering Research Council of Canada (NSERC) Silicon Electronic-Photonic Integrated Circuits (SiEPIC) Program. The devices were fabricated by Richard Bojko at the University of Washington Washington Nanofabrication Facility, part of the National Science Foundation's National Nanotechnology Infrastructure Network (NNIN), and Cameron Horvath at Applied Nanotools, Inc. Omid Esmaeeli performed the measurements at The University of British Columbia. I acknowledge Lumerical Solutions, Inc., Mathworks, Mentor Graphics, Python, and KLayout for the design software.

References

1.Lukas Chrostowski, Michael Hochberg. Silicon Photonics Design. Cambridge University Press (CUP), 2015. Link

2.Lukas Chrostowski, Michael Hochberg. Testing and packaging. 381–405 In Silicon Photonics Design. Cambridge University Press (CUP) Link

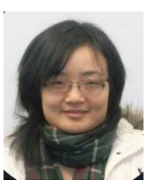

Xia Fang is a Senior Process Integration Engineer at GlobalFoundries, specializing in Back-End-of_Line (BEOL) integration for both technology transfer and fabrication process improvement. Piro to joining GlobalFoundries, Xia spent over ten years in the fiber optics industry/academia, developing a strong foundation in optical devices and laser design, characterization, testing ,and system-level development.